






Optimal strategy for multiple-phase estimation under practical measurement with multimode NOON states

Junaid ur Rehman ^{1,2,3,*} Seongjin Hong ^{1,*} Seung-Woo Lee,¹ Yong-Su Kim,^{1,4} Young-Wook Cho ^{1,5} Hojoong Jung,¹ Sung Moon,^{1,4} Hyundong Shin ² Sang-Wook Han,^{1,4} and Hyang-Tag Lim ^{1,4,†}

¹Center for Quantum Information, Korea Institute of Science and Technology, Seoul, 02792, Korea

²Department of Electronics and Information Convergence Engineering, Kyung Hee University, Yongin, 17104, Korea

³Interdisciplinary Centre for Security, Reliability and Trust, University of Luxembourg, L-1855, Luxembourg

⁴Division of Nano and Information Technology, Korea Institute of Science and Technology School, Korea University of Science and Technology, Seoul, 02792, Korea

⁵Department of Physics, Yonsei University, Seoul 03722, Korea



(Received 15 May 2022; accepted 29 August 2022; published 21 September 2022)

Quantum multiple parameter estimation can achieve an enhanced sensitivity beyond the classical limit. Although a theoretical ultimate sensitivity bound for multiple phase estimation is given by the quantum Cramer-Rao bound (QCRB), experimental implementations to saturate the QCRB typically require an impractical setup including entangled measurements. Since it is experimentally challenging to implement an entangled measurement, the practical sensitivity is given by the Cramer-Rao bound (CRB) relevant to the measurement probabilities. Here, we consider the problem of practical sensitivity bound for multiple phase estimation with quantum probe states and a measurement setup without entanglement, which consists of a beam splitter followed by the photon-number-resolving measurement. In this practical measurement scheme, we show that lower CRB can be achieved with a quantum probe state even with higher QCRB.

DOI: [10.1103/PhysRevA.106.032612](https://doi.org/10.1103/PhysRevA.106.032612)

I. INTRODUCTION

Quantum metrology is a promising quantum technology, which offers a sensitivity outperforming a classical metrology in a parameter estimation [1,2]. While a single parameter estimation has been widely studied [3–5], recent progress extended the scope of quantum metrology to the simultaneous estimation of multiple parameters [6–21]. The main motivation for this extension is the improved sensitivity in terms of quality of estimates as compared to individual estimation of each parameter by utilizing the same number of total resources [22,23].

For a single parameter estimation, the fundamental limit is given by the quantum Cramer-Rao bound (QCRB) [24,25], which can be saturated by a NOON state due to its largest number variance between the two modes [3–5]. However, for a multiple parameter estimation, the fundamental limit (QCRB) on the sensitivity is given by a matrix inequality between the quantum Fisher information matrix (QFIM) and the covariance matrix of the estimates [22,26,27]. It was shown that the multimode NOON states are optimal in multiple parameter estimation due to their lowest value of the QCRB [2,22,28–32].

However, the QFIM, and consequently the QCRB, are independent of the measurement setting employed in a metrological setup. This makes the saturation of the QCRB in

multiple parameter estimation scenario highly nontrivial as one needs to find the optimal measurements, if they exist, to extract all the information encoded in the probe states. Although, the existence of optimal measurements was found, the resulting measurements might still be experimentally difficult or even outright infeasible [27]. Then, the design of experimentally feasible measurement settings that allow to *achieve* the best sensitivity becomes more important and crucial in practical applications. That is, a feasible experimental setup with the best achievable sensitivity is more desirable than a setup with the lowest QCRB, but experimentally challenging or infeasible. The achievable sensitivity of a setup is characterized by the classical Cramér-Rao bound (CRB), which takes into account measurement statistics as well as the probe state [27,32,33].

In this work, we consider the simultaneous estimation of d unknown phases in an m -mode ($m = d + 1$) interferometric experimental setup with limited resources, i.e., limited photon number. Here, we analyze the QCRB and the CRB with three different probe states: coherent states as a classical strategy, single-photon Fock states, and multimode NOON states with limited photon number. In particular, for multimode NOON states, instead of optimizing the QCRB and then finding an optimal measurement setting of interferometric phase estimation, we fix a realistic measurement setting and then optimize the input probe states for this particular measurement. The measurement setting we consider is an $m \times m$ balanced beam-splitter (BS) followed by a photon number resolving (PNR) measurement. We first begin with the classical case with coherent states as a classical comparison. Then we consider

*These authors contributed equally to this work.

†hyangtag.lim@kist.re.kr

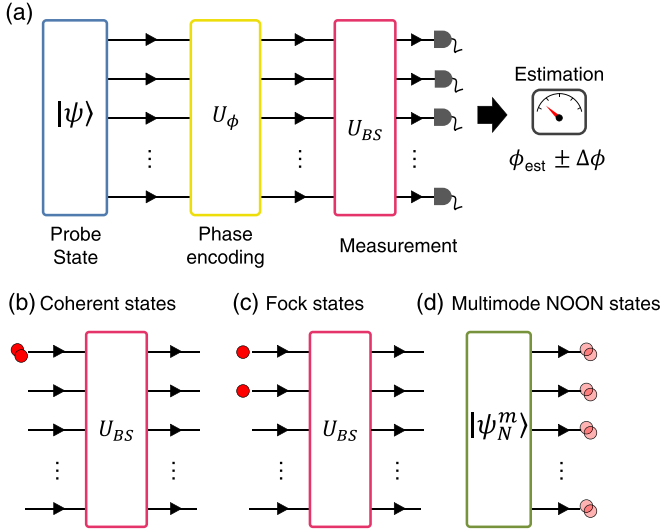


FIG. 1. (a) General scheme for multiple phases estimation. (b) A coherent state is inserted in one mode of U_{BS} . (c) Generation of $|\psi_{\text{Fock}}\rangle$ is achieved by exciting two modes of U_{BS} . (d) A generalized multimode NOON state occupies the i th output mode of U_{BS} with probability $|\alpha_i|^2$.

single-photon Fock states in two distinct modes and obtain its sensitivity bound. Then, we utilize the general multimode NOON states that are known to be optimal in terms of the QCRB and optimize them for our measurement setting. We find that a lower QCRB cannot guarantee better practical sensitivity considering a realistic measurement. Finally, we introduce a tunable unbalanced BS in our measurement and optimize both the input probe state and the split ratio of the BS. In this measurement setup, we find that a better practical sensitivity can be achieved with quantum probe state even with worse QCRB.

The remainder of this article is organized as follows. In Sec. II we describe our general scheme. In Sec. III, we provide examples of quantum metrology with a balanced BS and derive the QFIM and classical Fisher information matrix (CFIM) for single-photon Fock state in two excite modes and generalized multimode NOON state, respectively. This is followed by Sec. IV, where we derive the output state of an unbalanced BS. Finally, we conclude in Sec. V and discuss interesting potential future directions.

II. GENERAL SCHEME

Let us begin by introducing simultaneous multiple phase estimation for $\phi = \{\phi_0, \phi_1, \dots, \phi_d\}$, where $\phi_0 = 0$ serves as the reference phase and d unknown phases $\phi_j \in [0, 2\pi]$ for $1 \leq j \leq d$. We utilize the $m \times m$ multimode interferometric phase estimation scheme, with $m = d + 1$, as shown in Fig. 1(a). In general, the quantum-enhanced multiple phase estimation scheme consists of three steps: (i) preparation of quantum probe state; (ii) interaction with unknown phases ϕ ; and (iii) measurements. First, the probe state $|\psi_{\text{in}}\rangle$ is prepared and the phases ϕ are encoded in the probe state with phase encoding unitary transformation U_ϕ . Then the phase encoded state becomes $|\psi_\phi\rangle = U_\phi|\psi_{\text{in}}\rangle$. Finally, $|\psi_\phi\rangle$ is mea-

sured to infer the transformed state. These three steps are repeated μ times to construct statistics of measurement results. This quantum part is followed by a postprocessing step, where the estimated $\hat{\phi}$ of the vector of phases ϕ is obtained using appropriate estimators such as maximum likelihood estimation (MLE) and Bayesian estimation over measurement data [30,34,35].

For an unbiased estimator, the total variance for multiple phase estimation is given by the CRB and the QCRB as follows [31]:

$$\sum_{j=1}^d |\Delta\phi_j|^2 \geq \frac{\text{Tr}[F_C^{-1}(\phi)]}{\mu} \geq \frac{\text{Tr}[F_Q^{-1}(\phi)]}{\mu}, \quad (1)$$

where $|\Delta\phi_j|^2$ is the variance in the estimates of ϕ_j , $F_C(\phi)$ is the CFIM whose (j, k) th entry is

$$F_{C(j,k)} = \sum_{\ell} \frac{1}{P_{\ell}} \left(\frac{\partial P_{\ell}}{\partial \phi_j} \right) \left(\frac{\partial P_{\ell}}{\partial \phi_k} \right), \quad (2)$$

where P_{ℓ} is the probability of obtaining measurement result ℓ , and $F_Q(\phi)$ is the QFIM whose (j, k) th entry is defined as

$$F_{Q(j,k)} = 4 \text{Re} \{ \langle \partial_{\phi_j} \psi | \partial_{\phi_k} \psi \rangle - \langle \partial_{\phi_j} \psi | \psi \rangle \langle \psi | \partial_{\phi_k} \psi \rangle \}, \quad (3)$$

for a pure probe state $|\psi\rangle$.

The first inequality in Eq. (1) defines the CRB and the second defines the QCRB. It can be seen from the expressions for F_Q and F_C that QFIM depends only on the phase-encoded state whereas the CFIM depends on the measurement statistics, i.e., the set of all P_{ℓ} . Note that P_{ℓ} , in turn, is dependent on the phased-encoded state as well as the employed measurement scheme. Hence, to achieve the maximum sensitivity, it is important to optimize the probe state, which gives the lowest QCRB, and finding an optimal measurement scheme to saturate the QCRB. For the probe states, the multimode NOON states were shown to provide a better sensitivity than other quantum probe states [22,32], i.e., they provide a lower QCRB. However, a practical implementation of an optimal measurement to saturate the QCRB is highly challenging considering a realistic measurement scheme since it requires quantum-correlated measurements and *a priori* knowledge of the encoded phases [22,27,32]. It indicates that the QCRB cannot always be saturated under a practical measurement scheme.

This motivates us to consider a realistic measurement setting as shown in Fig. 1(a), and then optimize the tunable components such as probe states and/or split ratios of the BS before measurement to achieve the highest sensitivity. In this work, we mainly explore three possible candidate probe states for multiple phase estimation and compare them to a coherent state, which is a classical probe states with limited photon number $N = 2$. First, we consider a coherent state to show the quantum enhancement as a classical probe state as shown in Fig. 1(b). Then we explore a single-photon Fock state as shown in Fig. 1(c), where two input modes of an $m \times m$ BS are excited by single-photon Fock states [35], i.e.,

$$|\psi_{\text{Fock}}\rangle = |x_0, x_1, \dots, x_d\rangle,$$

where $x_j = x_k = 1$ for any two $j \neq k$, and $x_{\ell} = 0$, otherwise. The last probe state that we consider here is the

generalized multimode NOON state of the form as shown in Fig. 1(c) [22,32]

$$|\psi_N^d\rangle = \alpha_0 |N, 0, \dots, 0\rangle + \alpha_1 |0, N, 0, \dots, 0\rangle + \dots + \alpha_d |0, \dots, 0, N\rangle, \quad (4)$$

where $\alpha_k \in \mathbb{R}$ are the tunable probability amplitudes. Our measurement setup consists of a tunable multimode BS followed by a PNR detector as shown in Fig. 1(a). In the following section, we investigate the sensitivity bound of our multimode BS with an equal split ratio in each mode.

III. OPTIMIZATION OF PROBE STATES

In this section, we investigate the sensitivity bound of system shown in Fig. 1, i.e., multiple phase estimation where the phase encoding unitary U_ϕ is followed by an $m \times m$ balanced BS. We first derive the input-output relation of this system when the input probe state in experimental scheme as shown in Fig. 1. Note that we consider the limited resources with photon number $\bar{N} = 2$. We denote by $|\psi_{\text{QN}}\rangle$, the QCRB-optimized NOON state of [22]. The CRB-optimized NOON state that we obtain here is denoted by $|\psi_{\text{CN}}\rangle$. Furthermore, we use $|\Delta\phi_j|^2$ to denote the fundamental limit, i.e., the QCRB value, of variance in estimating ϕ_j . In the multiple phases setting, we use $|\Delta_Q|^2 \equiv \sum_j |\Delta\phi_j|^2 = \text{Tr}[F_Q^{-1}]$ to denote the total variance. We use $|\Delta_Q|^2$ as the main figure of merit in evaluating the quality of multiple phase estimation setup.

A. Coherent states

We consider a coherent state as a classical probe state. The coherent states are the eigenstates of annihilation operators and are important in quantum information processing [36]. A coherent state with mean photon number $\bar{N} = |\alpha|^2$ is defined as

$$|\alpha\rangle = e^{-\frac{|\alpha|^2}{2}} \sum_{n=0}^{\infty} \frac{\alpha^n}{\sqrt{n!}} |n\rangle, \quad (5)$$

where $\alpha \in \mathbb{C}$, and $|n\rangle$ is the n th Fock basis state. In a dynamical system, coherent states are the most classical of all states. Thus, they provide no quantum enhancement in sensitivity. Here, we investigate the sensitivity of Fock states with distinguishable single photons when coherent states are inserted in one of the input ports of the multimode BS. The coherent state $|\alpha\rangle$ with $\bar{N} = |\alpha|^2 = 2$ can be considered as two distinguishable photons at the first input port of multimode BS in Fig. 1(b).

Here, we give the QFIM for Fig. 1(b), when the input state is the single-photon Fock states in the first input port of the multimode BS with photon number $N = 1$, i.e., in the Fock basis we have

$$|\Psi_{\text{in}}\rangle = |1, 0, \dots, 0\rangle.$$

The CFIM of a single-photon Fock state can be obtained by plugging the last expression into Eq. (2). The QFIM of this

state can be obtained as

$$F_Q = 4 \begin{bmatrix} \frac{1}{m} - \frac{1}{m^2} & -\frac{1}{m^2} & \dots & -\frac{1}{m^2} \\ -\frac{1}{m^2} & \frac{1}{m} - \frac{1}{m^2} & \dots & -\frac{1}{m^2} \\ \vdots & \vdots & \ddots & \vdots \\ -\frac{1}{m^2} & -\frac{1}{m^2} & \dots & \frac{1}{m} - \frac{1}{m^2} \end{bmatrix}. \quad (6)$$

The total variance ($|\Delta_Q|^2 = \text{Tr}[F_Q^{-1}]$) of this system is $m(m+1)/2$. We calculate the QCRB and the CRB with single-mode Fock state. Since the coherent state $|\alpha\rangle$ with $\bar{N} = |\alpha|^2 = 2$ can be considered as two distinguishable photons, the sensitivity bounds of coherent states with $\bar{N} = 2$ are equivalent to the values of the CRB and the QCRB from $|1, 0, \dots, 0\rangle$ multiplied $1/2$ when $N = 2$, i.e., $m(m+1)/4$.

B. Single-photon Fock state

Here, we give the QFIM for Fig. 1(c), when the input state is the two-mode single-photon Fock states in two modes with limited photon number $N = 2$, i.e., in the Fock basis we have

$$|\Psi_{\text{in}}\rangle = |x_0, x_1, \dots, x_d\rangle$$

where $x_j = x_k = 1$ for any two $j \neq k$, and $x_\ell = 0$, otherwise.

For a pure state $|\psi\rangle$, the (y, z) th entry of the QFIM is given by Eq. (3). Since the QFIM is invariant under the action of a parameter-independent unitary, we can ignore the final BS, and obtain the QFIM at the output of the parameter encoding unitary U_ϕ . With this simplification, we can obtain (detailed derivation is given in Appendix B) the QFIM as

$$F_{Q(y,z)} = \begin{cases} \frac{8}{m}, & \text{if } y = z, \\ \frac{8}{m^2} \{ \cos[\frac{2\pi}{m}(j-k)(y-z)] - 1 \}, & \text{otherwise,} \end{cases} \quad (7)$$

where j and k are the two excited modes. Setting $j - k = 1$, we find the total variance to be

$$|\Delta_Q|^2 = \sum_{j=1}^d |\Delta\phi_j|^2 = \begin{cases} \frac{1}{4}, & \text{if } m = 2, \\ \frac{m(m-1)}{4} - \frac{m}{6}, & \text{otherwise.} \end{cases} \quad (8)$$

The CFIM for this setup can be obtained numerically from Eq. (2), by fixing some input modes j, k and utilizing the input-output relations of Fig. 1 derived in Appendix A. Bound on the total variance both by the QCRB and the CRB are shown in Fig. 2.

C. Multimode NOON states

Since it is not always possible to saturate the QCRB under realistic measurement settings [27], it is essential to evaluate the CRB of the implemented measurement setup. The QCRB with multimode NOON states is given in Ref. [22]. Here, we calculate the CRB of this setup with multimode NOON states. The CRB bounds the achievable sensitivity limit of a given phases estimation setup including the phase encoding and the measurement statistics. We derive the CFIM at the output of an $m \times m$ BS when its input ports are excited by

$$|\psi_{\text{in}}\rangle = \sum_{j=0}^d \alpha_j e^{iN\phi_j} \frac{(a_j^\dagger)^N}{\sqrt{N!}}, \quad (9)$$

where as before $\phi = \{\phi_1, \phi_2, \dots, \phi_d\}$ are the phases to be estimated. We obtain the CFIM of this scheme to be (detailed derivation is given in Appendix C)

$$F_{C(h,k)} = \sum_{\vec{x}} \frac{1}{P_{\vec{x}}} \left(\frac{\partial P_{\vec{x}}}{\partial \phi_h} \right) \left(\frac{\partial P_{\vec{x}}}{\partial \phi_k} \right) \\ = \frac{4\alpha_h \alpha_k N^2}{N! m^N} \sum_{\vec{x}} n^2(\vec{x}) b^2(\vec{x}) \frac{\sum_{j,\ell} \alpha_j \alpha_\ell \sin [N(\phi_j - \phi_h) + \frac{2\pi}{d} c(\vec{x})(j-h)] \sin [N(\phi_\ell - \phi_k) + \frac{2\pi}{d} c(\vec{x})(\ell-k)]}{1 + \sum_{j,\ell} \cos [N(\phi_\ell - \phi_j) + \frac{2\pi}{d} c(\vec{x})(\ell-j)]}, \quad (10)$$

where $\vec{x} \in \{0, 1, \dots, N\}^m$, s.t. $\sum \vec{x} = N$: Possible output vector, e.g., $[1, 0, 2]$ for 1 photon in 0 mode, 0 photons in mode 1, and 2 photons in mode 2. $n(\vec{x})$ number of possible configurations of creations operators of output mode that all create the output vector \vec{x} . $b(\vec{x}) = \sqrt{\prod_{j=0}^d \vec{x}(j)!}$ and $c(\vec{x}) = \sum_{j=0}^d j\vec{x}(j)$.

From Eq. (10), it is possible to numerically optimize the total variance $\sum |\Delta\phi|^2$ by varying the parameters α_j while satisfying the constraint $\sum_j |\alpha_j|^2 = 1$. We perform the numerical optimization for $N = 2$ and $d = 1, 2, 3, 4$. The resulting CRB-optimized NOON states are denoted by $|\psi_{CN}\rangle$. We plot the CRB and the QCRB of these states in Fig. 2. For comparison we also plot the CRB and the QCRB of QCRB-optimized NOON states of [22], denoted by $|\psi_{QN}\rangle$, two-mode single-photon Fock states $|\psi_{\text{Fock}}\rangle$, and coherent states with $\bar{N} = 2$ $|\psi_{\text{coh}}\rangle$. Here, note that $|\psi_{QN}\rangle$ is defined with $\alpha_j = 1/\sqrt{d + \sqrt{d}}$ for $j \neq 0$ and $\alpha_0^2 + d \sum_{j=1}^d \alpha_j^2 = 1$, and it gives the $|\Delta\phi|^2 = (m-1)(\sqrt{m-1} + 1)^2/4N^2$ [22]. From Fig. 2, it is clear that $|\psi_{CN}\rangle$ provides the lowest CRB value, achievable with the proposed practical setup.

In Fig. 3, we plot the total variance $\sum |\Delta\phi|^2$ of multiple phase estimation with $|\psi_{QN}\rangle$ and $|\psi_{CN}\rangle$ for different values of d with $N = 3$ in Fig. 3(a) and for different values of N with $d = 2$ in Fig. 3(b). It is clear from Fig. 3 that, despite an inferior sensitivity limit as predicted by the QCRB, $|\psi_{CN}\rangle$ outperforms $|\psi_{QN}\rangle$ in terms of the CRB. This shows that the

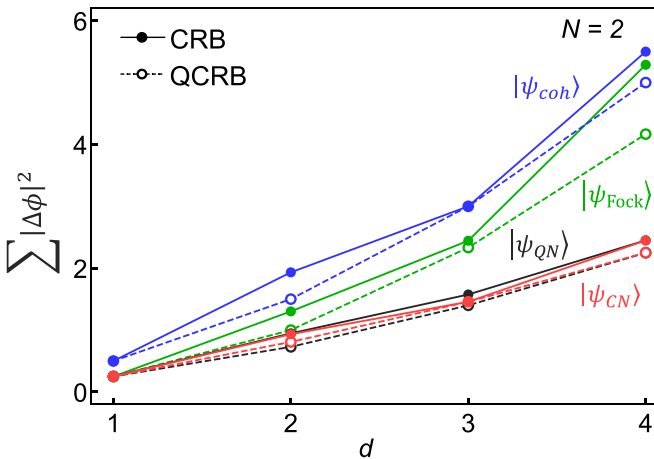


FIG. 2. Total variance of multiple phase estimation with different probe states. Here, $|\psi_{CN}\rangle$ denotes the CRB-optimized NOON state, $|\psi_{QN}\rangle$ denotes the QCRB-optimized NOON state in [22], $|\psi_{\text{Fock}}\rangle$ is the single-photon Fock state in two modes, and $|\psi_{\text{coh}}\rangle$ is the coherent state with $\bar{N} = 2$.

achievable sensitivity with $|\psi_{CN}\rangle$ is better than that with $|\psi_{QN}\rangle$ in the proposed measurement setup.

IV. OPTIMIZATION OF MEASUREMENTS

By comparing the CRB and the QCRB with different probe states, we find that the multimode NOON states give better sensitivity than other probe states. In addition, by comparing the QFIM and CFIM of multimode NOON states, it is clear that this setup fails to achieve the QCRB. In principle, one can construct a set of measurements that can saturate the QCRB. However, these measurements are generally difficult to implement practically as they are entangled and/or dependent on the phases. More critically, the optimal probe states that minimize the QCRB not necessarily minimize the CRB for a given measurement setting. In such situations, it is more appropriate to optimize the probe states for practical measurement settings.

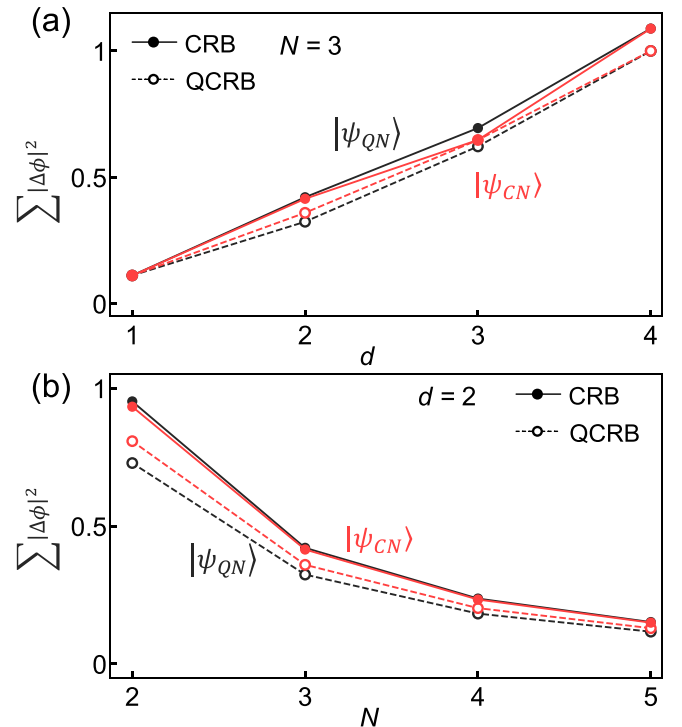


FIG. 3. Total variance of multiple phase estimation with different probe states. We compare the total variance $|\Delta\phi|^2$ of $|\psi_{CN}\rangle$ and $|\psi_{QN}\rangle$ for (a) different values of d with $N = 3$ and (b) different values of N with $d = 2$.

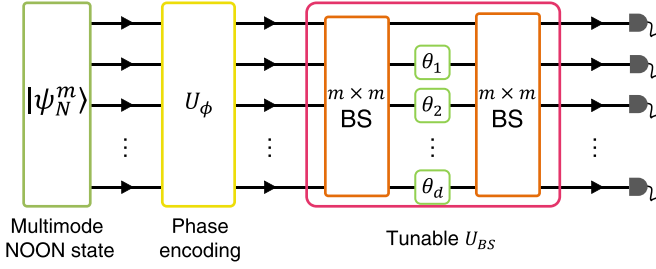


FIG. 4. Experimental scheme for multiple phase estimation with a split-ratio tunable multimode BS. A $m \times m$ unbalanced BS is shown. Split ratio of this component can be tuned by varying the phases θ_j .

From the results of Appendix A, the input-output relation of a multimode BS with single-photon Fock state input is given by

$$A_{k,\ell} = \frac{1}{m} \sum_{j=0}^d \exp \left[-i \left(\phi_j + \frac{2\pi j(k+\ell)}{m} \right) \right]. \quad (11)$$

This setup can also be used as an unbalanced BS whose split ratio can be tuned by changing the values of θ_k [37]. Figure 4 shows the multiple phase estimation setup with an unbalanced BS. The split ratio denotes the ratio of intensity of the output ports when only the first input is excited. For example, in the case of a tritter, the split ratio is $a : b : c$, where the a , b , and c are the fractions of photons leaving the first, second, and third output ports when the input is fed only in the first input port. Mathematically, the fraction T_j of photons leaving port j in this setting can be obtained as

$$T_j = A_{0,j} A_{0,j}^* \quad (12)$$

$$= \frac{1}{m^2} \sum_{k=0}^d \sum_{k'=0}^d \exp \left[i \left(\theta_{k'} - \theta_k + \frac{2\pi j}{m} (k' - k) \right) \right] \quad (13)$$

$$= \frac{1}{m^2} \left[m + 2 \sum_{k=0}^d \sum_{k' < k} \cos \left(\theta_{k'} - \theta_k + \frac{2\pi j}{m} (k' - k) \right) \right]. \quad (14)$$

Note that we use θ_k to denote the phases when used for tuning the split ratio of an unbalanced BS. By varying the values of θ_k , we can control the split ratio. For example, setting $\theta_k = \theta_j$ for all k and j , we get $T_0 = 1$ and $T_j = 0$ for all $j \neq 0$ for arbitrary d . For $m = 2$, setting $\theta_0 = 0$ and $\theta_1 = \pi/2$ gives 50:50 split ratio. Clearly, an unbalanced BS is a passive and lossless elements since $\sum_j T_j = 1$.

Now we derive the probability amplitudes at the output of an unbalanced BS which is excited by the input state of the form

$$\Psi^\dagger |0\rangle = \frac{1}{\sqrt{N!}} \sum_{\ell=0}^d \alpha_\ell e^{-iN\phi_\ell} (a_\ell^\dagger)^N |0\rangle, \quad (15)$$

i.e., an m -mode generalized NOON state where the phases of interest ϕ_ℓ are modulated by a unitary phases encoding. Then,

TABLE I. Minimum QCRB and CRB values depending on probability amplitudes of input states and split ratios of a BS with $N = 2$ and $d = 2$.

Probe state	BS	QCRB	CRB
$ \psi_{\text{QN}}\rangle$	Balanced	0.729	0.947
$ \psi_{\text{CN}}\rangle$	Balanced	0.808	0.933
$ \psi_{\text{BN}}\rangle$	Unbalanced	0.75	0.844

we have

$$(a_\ell^\dagger)^N = \sum_{j_1, j_2, \dots, j_N} A_{\ell, j_1} A_{\ell, j_2} \cdots A_{\ell, j_N} b_{j_1}^\dagger b_{j_2}^\dagger \cdots b_{j_N}^\dagger. \quad (16)$$

Utilizing Eq. (11), we get

$$(a_\ell^\dagger)^N = \frac{1}{m^N} \sum_{\vec{j}} \sum_{\vec{k}} \exp \left[-i \left(\sum_{h=1}^N \theta_{k_h} + \frac{2\pi}{m} \sum_{h=1}^N k_h (\ell + j_h) \right) \right] b_{\vec{j}}^\dagger, \quad (17)$$

where the summation over $\vec{j} = \{j_1, j_2, \dots, j_N\}$ should be understood as the individual summation over its components and $b_{\vec{j}}^\dagger = b_{j_1}^\dagger b_{j_2}^\dagger \cdots b_{j_N}^\dagger$.

Substituting Eq. (17) into Eq. (15), we get the probability amplitudes of system output as

$$\Psi^\dagger |0\rangle = \frac{1}{\sqrt{N!} m^N} \sum_{\ell=0}^d \sum_{\vec{j}} \sum_{\vec{k}} \exp \left[-i \left(\sum_{h=1}^N \theta_{k_h} + N\phi_\ell + \frac{2\pi}{m} \sum_{h=1}^N k_h (\ell + j_h) \right) \right] b_{\vec{j}}^\dagger |0\rangle. \quad (18)$$

Any further simplification of this expression seems cumbersome. However, numerical calculations can be carried out to obtain the total variance for different values of N and d .

In Table I, the QCRB and the CRB with $N = 2$ and $d = 2$ for different configurations of input probe states and measurement settings are provided. Here, $|\psi_{\text{BN}}\rangle$ is the balanced NOON state, which has the same amplitude [32]. It is clear from Table I that both $|\psi_{\text{CN}}\rangle$ and $|\psi_{\text{BN}}\rangle$ provide better achievable sensitivity than $|\psi_{\text{QN}}\rangle$, which provides the lowest QCRB. Furthermore, the tunable split ratio of the unbalanced BS provides additional advantage with $|\psi_{\text{BN}}\rangle$ in the achievable precision.

V. CONCLUSION

In simultaneous quantum multiple parameter estimation, both quantum probe states and measurements are important to enhance the sensitivity. While multimode NOON states are considered as an optimal state to have the maximum QCRB, the practical sensitivity given by the CRB cannot be saturated to be QCRB under a realistic measurement scheme. Here we considered a multiple phase estimation scenario with multimode NOON states under a practical measurement setting. We fixed the measurement scheme for estimating multiple phases estimation and compared the sensitivity bound of

different probe states. We found that the QCRB-optimized NOON states, $|\psi_{\text{QN}}\rangle$, fail to provide the best sensitivity in this setup. Instead, the probe states obtained by optimizing the CRB provide better sensitivity. This results establishes that the CRB is the correct figure-of-merit to choose the probe states in practical multiple phases estimation schemes. Our results can pave the way for various applications of multiple phase estimation to achieve the practical maximum sensitivity.

ACKNOWLEDGMENTS

This work was supported by the National Research Foundation of Korea (NRF) (Grants No. 2019M3E4A1079777, No. 2019R1A2C2007037, and No. 2021R1C1C1003625), the Institute for Information and Communications Technology Promotion (IITP) (Grant No. 2020-0-00947), and the KIST research program (Grant No. 2E31531).

APPENDIX A: INPUT-OUTPUT RELATIONS OF SYSTEM OF FIG. 1

Here, we derive the input–output relations of system of Fig. 1(a) with the single-photon Fock state as the input. In this setup, the photon can be input to any of the m input ports a_j , $j \in \{0, 1, \dots, d\}$. The input photon passes through an $m \times m$ BS U_{BS} , followed by a phases encoding unitary U_ϕ which encodes d phases $\phi_1, \phi_2, \dots, \phi_d$. The first arm of this setup is considered as a reference, thus setting $\phi_0 = 0$. Finally, the photon passes through another $m \times m$ BS before exiting this system to ports labeled by b_j , $j \in \{0, 1, \dots, m\}$. By deriving the input-output relations of this setup we mean to derive the probability $P_{j,k}$ of the photon leaving from b_k when it entered the port a_j .

The transfer matrices of the BS and the phases encoding unitaries are given by

$$[U_{\text{BS}}]_{j,k} = \frac{1}{\sqrt{m}}\omega^{jk} \text{ and } [U_\phi]_{j,k} = \delta_{jk}e^{i\phi_k},$$

respectively, with $\omega = e^{\frac{2\pi i}{m}}$, and $\phi_0 = 0$.

From system model,

$$\vec{b} = U_{\text{BS}} U_\phi U_{\text{BS}} \vec{a}.$$

Since all matrices are unitary, we have

$$\vec{a} = U_{\text{BS}}^\dagger U_\phi^\dagger U_{\text{BS}}^\dagger \vec{b}.$$

Using the matrix multiplication we get

$$[U_{\text{BS}}^\dagger U_\phi^\dagger]_{j,k} = \sum_{\ell=0}^d \frac{1}{\sqrt{m}}\omega^{-j\ell}\delta_{k\ell}e^{-i\phi_k} = \frac{1}{\sqrt{m}}\omega^{-jk}e^{-i\phi_k}.$$

Similarly,

$$\begin{aligned} [U_{\text{BS}}^\dagger U_\phi^\dagger U_{\text{BS}}^\dagger]_{j,k} &= \sum_{\ell=0}^d \frac{1}{\sqrt{m}}\omega^{-j\ell}e^{-i\phi_\ell} \frac{1}{\sqrt{m}}\omega^{-k\ell} \\ &= \frac{1}{m} \sum_{\ell=0}^d \exp\left[-i\left(\phi_\ell + \frac{2\pi\ell(j+k)}{m}\right)\right] \\ &= [A]_{j,k}. \end{aligned}$$

This last expression gives the probability *amplitude* of a photon at output mode k , when the input mode j is excited with a single photon. Let, $\phi_\ell + \frac{2\pi\ell(j+k)}{m} = \phi_\ell^{j,k}$. Then, the probability of photon exiting the output mode k when the input mode j is excited is given by

$$\begin{aligned} P_{i,j} &= [A]_{j,k} [A]_{j,k}^* \\ &= \frac{1}{m^2} \left[m + 2 \sum_{\ell=1}^d \cos \phi_\ell^{j,k} + 2 \sum_{\ell=1}^{h-1} \sum_{h=1}^d \cos(\phi_\ell^{j,k} - \phi_h^{j,k}) \right]. \end{aligned}$$

APPENDIX B: QFIM FOR TWO-EXCITED MODES' SINGLE-PHOTON FOCK STATE

We have

$$a_k^\dagger = \sum_{j=0}^d A_{k,j} b_j^\dagger,$$

where $A = U_\phi^\dagger U_{\text{BS}}^\dagger$, i.e.,

$$A_{k,j} = \frac{1}{\sqrt{m}} e^{-i(\phi_j + \frac{2\pi}{m}kj)}.$$

Let us excite two input modes, a_k and a_ℓ , then we can write

$$\begin{aligned} a_k^\dagger a_\ell^\dagger &= \frac{1}{2} \sum_{h,j} (A_{k,h} A_{\ell,j} + A_{k,j} A_{\ell,h}) b_h^\dagger b_j^\dagger \\ &= \frac{1}{2m} \sum_{h,j} e^{-i(\phi_h + \phi_j)} (e^{-i\frac{2\pi}{m}(kh + \ell j)} + e^{-i\frac{2\pi}{m}(kj + \ell h)}) b_h^\dagger b_j^\dagger. \end{aligned} \tag{B1}$$

The partial derivative $\partial/\partial\phi_y$ of Eq. (B1) is

$$\begin{aligned} \frac{\partial}{\partial\phi_y} a_k^\dagger a_\ell^\dagger &= \frac{1}{m} \sum_j -ie^{-i(\phi_j + \phi_y)} (e^{-i\frac{2\pi}{m}(kj + \ell y)} + e^{-i\frac{2\pi}{m}(ky + \ell j)}) b_j^\dagger b_y^\dagger. \end{aligned} \tag{B2}$$

The inner product between $\partial/\partial\phi_y$ of Eq. (B1) and $\partial/\partial\phi_z$ of Eq. (B1) is

$$\begin{aligned} \langle \partial_{\phi_z} \psi | \partial_{\phi_y} \psi \rangle &= \frac{2}{m^2} \left\{ \delta_{y,z} \sum_j \left[1 + \cos\left(\frac{2\pi}{m}(k - \ell)(j - y)\right) \right] f^2(j, y) \right. \\ &\quad \left. + (1 - \delta_{y,z}) \left[1 + \cos\left(\frac{2\pi}{m}(k - \ell)(z - y)\right) \right] \right\}, \end{aligned} \tag{B3}$$

where $f(j, k) = \sqrt{2}$ when $j = k$, and is equal to one otherwise.

Similarly,

$$\begin{aligned} \langle \partial_{\phi_y} \psi | \psi \rangle &= \frac{2i}{m^2} \left\{ \sum_j \left[1 + \cos\left(\frac{2\pi}{m}(k - \ell)(j - y)\right) \right] \right\} \\ &= \frac{2i}{m}. \end{aligned} \tag{B4}$$

Thus,

$$\langle \partial_{\phi_y} \psi | \psi \rangle \langle \psi | \partial_{\phi_z} \psi \rangle = \frac{4}{m^2}, \quad (\text{B5})$$

and we can calculate the quantum Fisher information matrix as

$$\mathcal{F}_{y,z} = \begin{cases} \frac{8}{m}, & \text{if } y = z, \\ \frac{8}{m^2} \{ \cos [\frac{2\pi}{m}(k - \ell)(y - z)] - 1 \}, & \text{otherwise.} \end{cases} \quad (\text{B6})$$

Setting $k - \ell = 1$, we find the total variance to be

$$|\Delta\phi_Q|^2 = \begin{cases} \frac{1}{4}, & \text{if } m = 2, \\ \frac{2m(m-1)}{8} - \frac{m}{6}, & \text{otherwise.} \end{cases} \quad (\text{B7})$$

APPENDIX C: CFIM FOR A MULTIMODE NOON STATE

Since the input-output relation of an $m \times m$ BS is

$$a_k^\dagger = \frac{1}{\sqrt{m}} \sum_{j=0}^d e^{i\frac{2\pi}{m}kj} b_j^\dagger,$$

we get

$$\begin{aligned} (a_k^\dagger)^N &= \frac{1}{m^{N/2}} \sum_{j_1} \sum_{j_2} \dots \sum_{j_N} e^{i\frac{2\pi}{m}(j_1 + \dots + j_N)} b_{j_1}^\dagger b_{j_2}^\dagger \dots b_{j_N}^\dagger \\ &= \frac{1}{m^{N/2}} \sum_{\vec{x}} B(\vec{x}) b_{\vec{x}}^\dagger, \end{aligned} \quad (\text{C1})$$

where \vec{x} is an m elements vector whose entries are nonnegative integers satisfying $\sum \vec{x} = N$ and correspond to the photon number configuration in the output ports. The summation is over all such vectors \vec{x} . The corresponding coefficient

$$B(\vec{x}) = n(\vec{x}) e^{i\frac{2\pi}{m} \sum_{j=0}^d j\vec{x}(j)},$$

where $n(\vec{x})$ is the total number of possible combinations of (j_1, j_2, \dots, j_N) such that $b_{j_1}^\dagger b_{j_2}^\dagger \dots b_{j_N}^\dagger$ generates $b_{\vec{x}}^\dagger$. Also, define

$$c(\vec{x}) = \sum_{j=0}^d j\vec{x}(j).$$

Plugging Eq. (C1) in Eq. (9), we get

$$\psi_{\text{in}} = \frac{1}{\sqrt{N!m^N}} \sum_{\vec{x}} n(\vec{x}) b_{\vec{x}}^\dagger \sum_{k=0}^d \alpha_k e^{i(N\phi_k + \frac{2\pi}{m}kc(\vec{x}))}. \quad (\text{C2})$$

For a fixed photon number configuration \vec{x} , the probability amplitude $A(\vec{x})$ is given by

$$A(\vec{x}) = \frac{1}{\sqrt{N!m^N}} n(\vec{x}) b(\vec{x}) \sum_{k=0}^d \alpha_k e^{i(N\phi_k + \frac{2\pi}{m}kc(\vec{x}))},$$

where $b(\vec{x})$ accounts for the normalization factor from higher (greater than 1) order creation operators [38].

The probability of output photon number configuration \vec{x} is given by

$$\begin{aligned} P(\vec{x}) &= A(\vec{x})A^*(\vec{x}) = \frac{1}{N!m^N} n^2(\vec{x}) b^2(\vec{x}) \sum_{k=0}^d \alpha_k e^{i(N\phi_k + \frac{2\pi}{m}kc(\vec{x}))} \sum_{j=0}^d \alpha_j^* e^{-i(N\phi_j + \frac{2\pi}{m}jc(\vec{x}))} \\ &= \frac{1}{N!m^N} n^2(\vec{x}) b^2(\vec{x}) \sum_{j,k} \alpha_k \alpha_j^* e^{i(N(\phi_k - \phi_j) + \frac{2\pi}{m}c(\vec{x})(k-j))} \\ &= \frac{1}{N!m^N} n^2(\vec{x}) b^2(\vec{x}) \left(1 + \frac{1}{2} \sum_{\substack{j,k \\ j \neq k}} \alpha_k \alpha_j^* (e^{i[N(\phi_k - \phi_j) + \frac{2\pi}{m}c(\vec{x})(k-j)]} + e^{-i[N(\phi_k - \phi_j) + \frac{2\pi}{m}c(\vec{x})(k-j)]}) \right) \\ &= \frac{1}{N!m^N} n^2(\vec{x}) b^2(\vec{x}) \left(1 + \sum_{\substack{j,k \\ j \neq k}} \alpha_k \alpha_j^* \cos \left(N(\phi_k - \phi_j) \frac{2\pi}{m} c(\vec{x})(k-j) \right) \right). \end{aligned}$$

Assuming $\alpha_j \in \mathbb{R}$ for all j and after some trigonometric and algebraic tricks, we can write the partial derivative $\partial P / \partial \phi_j$ as

$$\frac{\partial P(\vec{x})}{\partial \phi_j} = \frac{2N}{N!m^N} n^2(\vec{x}) b^2(\vec{x}) \sum_{k=0}^d \alpha_j \alpha_k \sin \left(N(\phi_k - \phi_j) + \frac{2\pi}{m} c(\vec{x})(k-j) \right),$$

from where we are finally able to obtain the explicit form of the CFIM given in Eq. (2)

$$\begin{aligned} F_{C(h,k)} &= \sum_{\vec{x}} \frac{1}{P_{\vec{x}}} \left(\frac{\partial P_{\vec{x}}}{\partial \phi_j} \right) \left(\frac{\partial P_{\vec{x}}}{\partial \phi_k} \right) \\ &= \frac{4\alpha_h \alpha_k N^2}{N!m^N} \sum_{\vec{x}} n^2(\vec{x}) b^2(\vec{x}) \frac{\sum_{j,\ell} \alpha_j \alpha_\ell \sin [N(\phi_j - \phi_h) + \frac{2\pi}{m}c(\vec{x})(j-h)] \sin [N(\phi_\ell - \phi_k) + \frac{2\pi}{m}c(\vec{x})(\ell-k)]}{1 + \sum_{j,\ell} \cos [N(\phi_\ell - \phi_j) + \frac{2\pi}{m}c(\vec{x})(\ell-j)]}, \end{aligned} \quad (\text{C3})$$

where

(1) $\vec{x} \in \{0, 1, \dots, N\}^m$, s.t. $\sum \vec{x} = N$: Possible output vector, e.g., $[1, 0, 2]$ for 1 photon in 0 mode, 0 photons in mode 1, and 2 photons in mode 2.

- (2) $n(\vec{x})$ number of possible configurations of creations operators of output mode that all create the output vector \vec{x} .
- (3) $b(\vec{x}) = \sqrt{\prod_{j=0}^d \vec{x}(j)!}$.
- (4) $c(\vec{x}) = \sum_{j=0}^d i\vec{x}(j)$.

-
- [1] S. Pirandola, B. R. Bardhan, T. Gehring, C. Weedbrook, and S. Lloyd, Advances in photonic quantum sensing, *Nat. Photonics* **12**, 724 (2018).
- [2] E. Polino, M. Valeri, N. Spagnolo, and F. Sciarrino, Photonic quantum metrology, *AVS Quantum Sci.* **2**, 024703 (2020).
- [3] J. P. Dowling, Quantum optical metrology—the lowdown on high-NOON states, *Contemp. Phys.* **49**, 125 (2008).
- [4] S. Slussarenko, M. M. Weston, H. M. Chrzanowski, L. K. Shalm, V. B. Verma, S. W. Nam, and G. J. Pryde, Unconditional violation of the shot-noise limit in photonic quantum metrology, *Nat. Photonics* **11**, 700 (2017).
- [5] C. You, M. Hong, P. Bierhorst, A. E. Lita, S. Glancy, S. Kolthammer, E. Knill, S. W. Nam, R. P. Mirin, O. S. Magaña-Loaiza *et al.*, Scalable multiphoton quantum metrology with neither pre-nor post-selected measurements, *Appl. Phys. Rev.* **8**, 041406 (2021).
- [6] X. Guo *et al.*, Distributed quantum sensing in a continuous-variable entangled network, *Nat. Phys.* **16**, 281 (2020).
- [7] L. Z. Liu *et al.*, Distributed quantum phase estimation with entangled photons, *Nat. Photonics* **15**, 137 (2021).
- [8] M. Jachura, R. Chrapkiewicz, R. Demkowicz-Dobrzański, W. Wasilewski, and K. Banaszek, Mode engineering for realistic quantum-enhanced interferometry, *Nat. Commun.* **7**, 11411 (2016).
- [9] M. D. Vidrighin *et al.*, Joint estimation of phase and phase diffusion for quantum metrology, *Nat. Commun.* **5**, 3532 (2014).
- [10] E. Roccia *et al.*, Multiparameter approach to quantum phase estimation with limited visibility, *Optica* **5**, 1171 (2018).
- [11] Z. Hou, J. F. Tang, H. Chen, H. Yuan, G. Y. Xiang, C. F. Li, and G. C. Guo, Zero-trade-off multiparameter quantum estimation via simultaneously saturating multiple heisenberg uncertainty relations, *Sci. Adv.* **7**, eabd2986 (2021).
- [12] P.-A. Moreau, E. Toninelli, T. Gregory, and M. J. Padgett, Imaging with quantum states of light, *Nat. Rev. Phys.* **1**, 367 (2019).
- [13] G. Brida, M. Genovese, and I. R. Berchera, Experimental realization of sub-shot-noise quantum imaging, *Nat. Photonics* **4**, 227 (2010).
- [14] J.-M. Cui, F.-W. Sun, X. D. Chen, Z.-J. Gong, and G.-C. Guo, Quantum Statistical Imaging of Particles without Restriction of the Diffraction Limit, *Phys. Rev. Lett.* **110**, 153901 (2013).
- [15] N. P. Mauranyapin, L. S. Madsen, M. A. Taylor, M. Waleed, and W. P. Bowen, Evanescent single-molecule biosensing with quantum-limited precision, *Nat. Photonics* **11**, 477 (2017).
- [16] T. Ono, R. Okamoto, and S. Takeuchi, An entanglement-enhanced microscope, *Nat. Commun.* **4**, 2426 (2013).
- [17] M. A. Taylor and W. P. Bowen, Quantum metrology and its application in biology, *Phys. Rep.* **615**, 1 (2016).
- [18] Y. Xia, W. Li, W. Clark, D. Hart, Q. Zhuang, and Z. Zhang, Demonstration of a Reconfigurable Entangled Radio-Frequency Photonic Sensor Network, *Phys. Rev. Lett.* **124**, 150502 (2020).
- [19] W. Ge, K. Jacobs, Z. Eldredge, A. V. Gorshkov, and M. Foss-Feig, Distributed Quantum Metrology with Linear Networks and Separable Inputs, *Phys. Rev. Lett.* **121**, 043604 (2018).
- [20] A. Z. Goldberg, I. Gianani, M. Barbieri, F. Sciarrino, A. M. Steinberg, and N. Spagnolo, Multiphase estimation without a reference mode, *Phys. Rev. A* **102**, 022230 (2020).
- [21] Z. Hou, Y. Jin, H. Chen, J.F. Tang, C. J. Huang, H. Yuan, G. Y. Xiang, C. F. Li, and G. C. Guo, “Super-Heisenberg” and Heisenberg Scalings Achieved Simultaneously in the Estimation of a Rotating Field, *Phys. Rev. Lett.* **126**, 070503 (2021).
- [22] P. C. Humphreys, M. Barbieri, A. Datta, and I. A. Walmsley, Quantum Enhanced Multiple Phase Estimation, *Phys. Rev. Lett.* **111**, 070403 (2013).
- [23] T. Baumgratz and A. Datta, Quantum Enhanced Estimation of a Multidimensional Field, *Phys. Rev. Lett.* **116**, 030801 (2016).
- [24] S. L. Braunstein, C. M. Caves, and G. J. Milburn, Generalized uncertainty relations: Theory, examples, and lorentz invariance, *Ann. Phys. (NY)* **247**, 135 (1996).
- [25] S. L. Braunstein and C. M. Caves, Statistical Distance and the Geometry of Quantum States, *Phys. Rev. Lett.* **72**, 3439 (1994).
- [26] M. Gessner, L. Pezzè, and A. Smerzi, Sensitivity Bounds for Multiparameter Quantum Metrology, *Phys. Rev. Lett.* **121**, 130503 (2018).
- [27] L. Pezze, M. A. Ciampini, N. Spagnolo, P. C. Humphreys, A. Datta, I. A. Walmsley, M. Barbieri, F. Sciarrino, and A. Smerzi, Optimal Measurements for Simultaneous Quantum Estimation of Multiple Phases, *Phys. Rev. Lett.* **119**, 130504 (2017).
- [28] L. Zhang and K. W. C. Chan, Quantum multiparameter estimation with generalized balanced multimode noon-like states, *Phys. Rev. A* **95**, 032321 (2017).
- [29] L. Zhang and K. W. C. Chan, Scalable generation of multi-mode noon states for quantum multiple-phase estimation, *Sci. Rep.* **8**, 11440 (2018).
- [30] V. Gebhart, A. Smerzi, and L. Pezzè, Bayesian Quantum Multiphase Estimation Algorithm, *Phys. Rev. Appl.* **16**, 014035 (2021).
- [31] J. Liu, H. Yuan, X. M. Lu, and X. Wang, Quantum fisher information matrix and multiparameter estimation, *J. Phys. A: Math. Theor.* **53**, 023001 (2020).
- [32] S. Hong, J. ur Rehman, Y.-S. Kim, Y.-W. Cho, S.-W. Lee, H. Jung, S. Moon, S.-W. Han, and H.-T. Lim, Quantum enhanced multiple-phase estimation with multi-mode NOON states, *Nat. Commun.* **12**, 5211 (2021).
- [33] S. Hong, J. ur Rehman, Y.-S. Kim, Y.-W. Cho, S.-W. Lee, S.-Y. Lee, and H.-T. Lim, Practical Sensitivity Bound for Multiple Phase Estimation with Multi-Mode NOON States, *Laser Photonics Rev.* **16**, 2100682 (2022).
- [34] N. Wiebe and C. Granade, Efficient Bayesian Phase Estimation, *Phys. Rev. Lett.* **117**, 010503 (2016).

- [35] E. Polino, M. Riva, M. Valeri, R. Silvestri, G. Corrielli, A. Crespi, N. Spagnolo, R. Osellame, and F. Sciarrino, Experimental multiphase estimation on a chip, *Optica* **6**, 288 (2019).
- [36] B. C. Sanders, Review of entangled coherent states, *J. Phys. A: Math. Theor.* **45**, 244002 (2012).
- [37] I. Kim, D. Lee, S. Hong, Y.-W. Cho, K. J. Lee, Y.-S. Kim, and H.-T. Lim, Implementation of a 3×3 directionally-unbiased linear optical multiport, *Opt. Express* **29**, 29527 (2021).
- [38] If a^\dagger is a creation operator then $(a^\dagger)^N |0\rangle = \sqrt{N!} |N\rangle$, where $\sqrt{N!}$ is the normalization factor. Factor $b(\vec{x})$ caters for this normalization for the entire state $|\vec{x}\rangle$.